

See discussions, stats, and author profiles for this publication at: <https://www.researchgate.net/publication/253702072>

# Surface drag

Article · June 2009

DOI: 10.1063/1.3179913

---

CITATIONS

0

---

READS

429

4 authors, including:



**Murilo Almeida**

Universidade Federal do Ceará

49 PUBLICATIONS 1,463 CITATIONS

[SEE PROFILE](#)



**Eric Parteli**

University of Duisburg-Essen

114 PUBLICATIONS 4,001 CITATIONS

[SEE PROFILE](#)

# Surface drag

Hans J. Herrmann<sup>\*,†</sup>, Murilo P. Almeida<sup>†</sup>, Eric J. R. Parteli<sup>†</sup> and José S. Andrade Jr.<sup>†,\*</sup>

<sup>\*</sup>Computational Physics, IfB, ETH Zürich, Schafmattstr. 6, 8093 Zürich, Switzerland

<sup>†</sup>Departamento de Física, Universidade Federal do Ceará - 60455-760, Fortaleza, CE, Brazil

**Abstract.** I will discuss the drag of particles on granular surfaces by a fluid. I will present simulations using FLUENT of Aeolian saltation under Earth and Mars conditions obtaining among others the static and dynamic threshold shear and the height of the saltation layer as function of the wind strength. A universal quadratic increase of the saturated flux as function of the difference from the threshold is established.

**Keywords:** aeolian transport | critical phenomena | Mars | saltation

**PACS:** 45.70.Mg, 47.55.Kf, 47.27.-i, 83.80.Hj

## INTRODUCTION

The motion of sand grains in a sequence of ballistic trajectories close to the ground is called saltation and is a major factor for surface erosion, dune formation and triggering of dust storms on Mars. Although this mode of sand transport has been matter of research for decades both through simulations and wind tunnel experiments under Earth and Mars conditions, it has not been possible to provide accurate measurements of particle trajectories in fully developed turbulent flow. Here we calculate the motion of saltating grains by directly solving the turbulent wind field and its interaction with the particles. On the basis of our results, we arrive at general expressions which can be applied to calculate the length and height of saltation trajectories and the flux of grains in saltation under different physical conditions, when the wind velocity is close to the minimal threshold for saltation. Our calculations show that the minimal wind velocity required to sustain saltation on Mars may be surprisingly lower than the aerodynamic minimal threshold measurable in wind tunnels. Indeed, Mars grains saltate in 100 times higher and longer trajectories and reach 5–10 times higher velocities than Earth grains do.

## THE MODEL

We simulate saltation by solving, first, the turbulent wind field inside a long two-dimensional channel (wind tunnel) and, next, the air feedback with the dragged particles. The details of the calculation procedure are described elsewhere [12]. The fluid (air) is incompressible and Newtonian, the Reynolds-averaged Navier-Stokes equations with the standard  $\kappa - \varepsilon$  model being employed to describe turbulence [13].

The turbulent wind is, first, calculated without particles. The wind is generated by a pressure difference imposed between the extremities of the tunnel [12] and achieves a stable profile, the wind velocity  $u(z)$  increasing with the height  $z$  as  $u(z) = 2.5u_* \log z/z_0$ , where  $z_0$  is the surface roughness ( $\approx 10^{-4}$  m) and  $u_*$ , the wind shear velocity, quantifies the wind strength [3]. Boundary conditions are zero wind velocity at the bottom wall and zero shear ( $u_* = 0$ ) at the upper wall (gravity  $g$  points downwards).

Once steady-state turbulent flow is produced, particles are injected from the inlet at the ejection angle of grain-bed collisions with a velocity of the order of 60 cm/s. Grain trajectories are obtained by integrating the equation of motion:

$$\frac{dv_p}{dt} = F_D(u - v_p) + g(\rho_p - \rho_{\text{fluid}})/\rho_p, \quad (1)$$

where  $v_p$  is the particle velocity,  $\rho_{\text{fluid}}$  and  $\rho_p$  the density of the fluid and of the particles, respectively, and  $F_D(u - v_p)$  represents the drag force per unit particle mass, where

$$F_D = \frac{18\eta}{\rho_p d^2} \frac{C_D \text{Re}}{24}, \quad (2)$$

$\text{Re} = \rho_{\text{fluid}} d |u - v_p| / \eta$  is the particle Reynolds number,  $d$  is the grain diameter,  $\eta$  the air viscosity and the drag coefficient  $C_D$  is taken from empirical relations [14]. The feedback on the local velocity of the fluid due to its momentum exchange with the particles is accounted for by adding the momentum change of every particle as it passes through a control volume [12],

$$F = \sum_{\text{particles}} F_D(u - v_p) \dot{m}_p \Delta t, \quad (3)$$

where  $\dot{m}_p$  is the mass flow rate of the particles and  $\Delta t$  the time step. Each time a particle hits the ground it loses

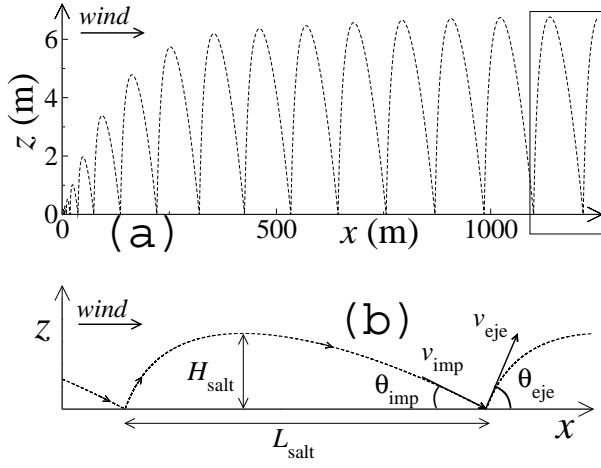


**FIGURE 1.** (a) The dashed line represents the trajectory of one saltating grain calculated using parameters for Mars with a wind strength of  $u_* = 1.78$  m/s. Gravity points downward (negative  $z$  direction) and the particle moves downwind, i.e. from left to right. In the absence of the saltating particles, the wind strength increases logarithmically with the height. However, the wind profile is disturbed by the saltating grains as shown in ref. [12]. (b) Typical saltation trajectory obtained in the calculations — the dashed line corresponds to the saltation path enclosed by the box in (a) — showing the velocity and angle of impact ( $v_{\text{imp}}$ ,  $\theta_{\text{imp}}$ ) and of ejection ( $v_{\text{eje}}$ ,  $\theta_{\text{eje}}$ ). The length  $L_{\text{salt}}$  and the maximum height  $H_{\text{salt}}$  of a saltation trajectory are also indicated in the figure.

a fraction  $r = 0.40$  of its momentum and a new stream of particles is ejected at that position with the ejection angle characteristic of saltation particles,  $\theta_{\text{eje}} = 36^\circ$  [5, 15]. The number of particle streams released,  $n_p$ , defines the sand flux  $q = \dot{m}_p n_p$ . Particle trajectories increase in height with the downwind position, achieving a maximum after a distance  $\Delta L$ , called “saturation length” [16], from the inlet. The saturated flux,  $q_s$ , is identified by the maximum number of particles streams,  $n_p$ , a wind of given strength  $u_*$  can transport without flux reducing due to energy loss of the trajectories [12].

In simulations for Earth, gravity  $g = 9.81$  m/s<sup>2</sup>, air viscosity  $\eta = 1.78 \times 10^{-5}$  kg·m<sup>-1</sup>s<sup>-1</sup> and density  $\rho_{\text{fluid}} = 1.225$  kg/m<sup>3</sup> are taken, while particle diameter  $d = 250$   $\mu$ m and density  $\rho_p = 2650$  kg/m<sup>3</sup> are as from sand of terrestrial dunes [3]. For Mars we use air density and viscosity  $\rho_{\text{fluid}} = 0.02$  kg/m<sup>3</sup>, respectively  $\eta = 1.3 \cdot 10^{-5}$  kg/m·s, while gravity is  $g = 3.71$  m/s<sup>2</sup> and Martian particles have diameter  $d = 600$   $\mu$ m and density  $\rho_p = 3200$  kg/m<sup>3</sup> typical of Martian dunes sand. Simulations are performed with  $u_*$  values between 0.27 m/s and 0.5 m/s for Earth and 1.12 m/s and 1.78 m/s for Mars, which means wind velocity values in the range  $u = 6.21 - 11.5$  m/s (Earth) and  $u = 25.8 - 41.0$  m/s (Mars) at a height of 1 m. Taking the wind velocity at this height, the fluid Reynolds number  $\text{Re}_f = u d \rho_{\text{fluid}} / \eta$  con-

sidered in the simulations is in the range 106.8 – 197.9 for Earth and 23.8 – 37.8 for Mars.

While Earth trajectories achieve the maximum height after typically  $\Delta L = 10$  m, Mars trajectories stabilize after  $\Delta L = 1.0$  km (fig. 1a), independently of  $u_*$ . Thus, the wind tunnel used in the simulations for Mars is much larger than the one used for Earth simulations (which has length 30 m and height 1.0 m), the former being 2.0 km long with a height of 10 m. We have performed simulations using channels of larger dimensions, both for Mars and for Earth. In both cases, it was found that increasing the size of the tunnel does not change the results.

## RESULTS AND DISCUSSION

In Figure 2 we show the increase of the resulting maximum flux of particles in saltation,  $q_s$ , with the shear velocity  $u_*$  on Mars. For comparison, the same simulations were performed using terrestrial atmospheric conditions and grain size and density characteristic of dunes on Earth (inset of fig. 1).

The scaling of the saturated flux with the shear velocity is universal:  $q_s \propto (u_* - u_{*t})^\alpha$ , where  $\alpha \approx 2.0$  is independent of the atmospheric conditions, and  $u_{*t}$ , the *impact threshold* wind velocity — the minimal wind velocity required to sustain the motion of saltating grains at saturation [3] — obtained in the simulations is around 1.12 m/s and 0.26 m/s on Mars and on Earth, respectively. As shown in a previous work [12], we have found a rather good agreement between the data obtained from our simulations for Earth and those obtained from field measurements by Lettau and Lettau [10], thus confirming the validity of our simulation procedure [12].

The flux of sand depends not only on the wind velocity but also on gravity, atmospheric and sand properties, which must be included in the coefficient of the scaling between  $q_s$  and  $u_*$ . One expression for  $q_s(u_*)$  which includes gravity and atmospheric density was proposed and validated through wind tunnel experiments under Earth and Mars air pressure conditions [4]. The simulations of the present work, however, reveal that the air viscosity also plays a relevant role in saltation, and cannot be neglected. If the ratio  $\rho_{\text{fluid}}/g$  is encoded in the coefficient of  $q_s(u_*)$  [4], then dimensional analysis requires a further term with units of velocity to be included into the scaling relation of fig. 2. Universality is only obtained when the nondimensional quantity  $d/l_v$  — where the length-scale  $l_v = (v^2/g)^{1/3}$  defines, together with the time-scale  $t_v = (v/g^2)^{1/3}$  the characteristic velocity  $v_v = l_v/t_v$ , with  $v = \eta/\rho_{\text{fluid}}$  — is incorporated into the prefactor of the sand flux equation. This quantity encodes the information of the amount of momen-

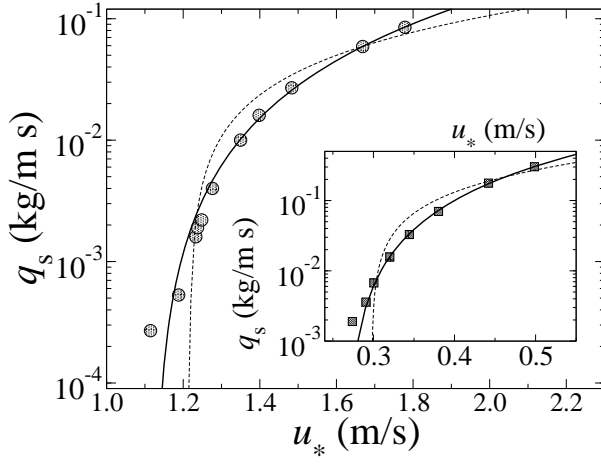


**FIGURE 2.** In the main plot, the circles show the saturated flux  $q_s$  calculated as function of the shear velocity  $u_*$  for Mars. The quadratic relation  $q_s \propto (u_* - u_{*t})^2$ , indicated by the full line, fits the data notoriously better than the classical equation for planetary sand flux [4] — whose corrected version reads [17]  $q_w = C[\rho_{\text{fluid}}/g]u_*^2(1 - u_{*t}/u_*)(1 + u_{*t}/u_*)^2$  (dashed line) — and gives  $u_{*t} = 1.12$  m/s for Mars. The range of shear velocities  $u_* = 1.12 - 1.78$  m/s used for Mars corresponds to shear stress  $\tau = \rho_{\text{fluid}}u_*^2$  values in the range  $0.025 - 0.063$  kg m<sup>-1</sup> s<sup>-2</sup>. The corresponding calculations for Earth are shown in the inset. In this case, simulations were performed with shear velocities in the range  $u_* = 0.27 - 0.5$  m/s.

tum lost due to the grain-bed collisions that has to be compensated by the drag force in the equilibrium [11]. A formula for the sand flux is then obtained, which can be applied to calculate  $q_s$  as function of  $u_*$  under arbitrary physical environments (fig. 3):

$$q_s \approx 227.3 \cdot \left[ d \rho_{\text{fluid}} / (v g)^{2/3} \right] \cdot u_{*t} \cdot (u_* - u_{*t})^2. \quad (4)$$

Both the length and height of the saltation paths increase linearly with the shear velocity  $u_*$ , when this is close to the threshold (fig. 4). Dimensional analysis leads to a scaling of  $H_{\text{salt}}$  and  $L_{\text{salt}}$  with  $t_v(u_* - u_{*t})$ . Using our data to obtain the respective constants of proportionality, we find that universal equations for  $L_{\text{salt}}$  and  $H_{\text{salt}}$  can be obtained if the quantity  $\sqrt{l_v/d}$  is incorporated into the coefficients of both saltation length and height. In this manner, we arrive at the following expressions, which can be used to predict the saltation trajectories under an arbitrary planetary surface, for  $u_*$  close to the threshold  $u_{*t}$ :

$$H_{\text{salt}} \approx 81.46 \cdot (v^2/g)^{1/3} \cdot (u_* - u_{*t}) / \sqrt{gd}, \quad (5)$$

$$L_{\text{salt}} \approx 1091.5 \cdot (v^2/g)^{1/3} \cdot (u_* - u_{*t}) / \sqrt{gd}, \quad (6)$$

where  $(v^2/g)^{1/3}$  is the characteristic lengthscale  $l_v$  and  $\sqrt{gd}$  represents the grain velocity necessary to escape

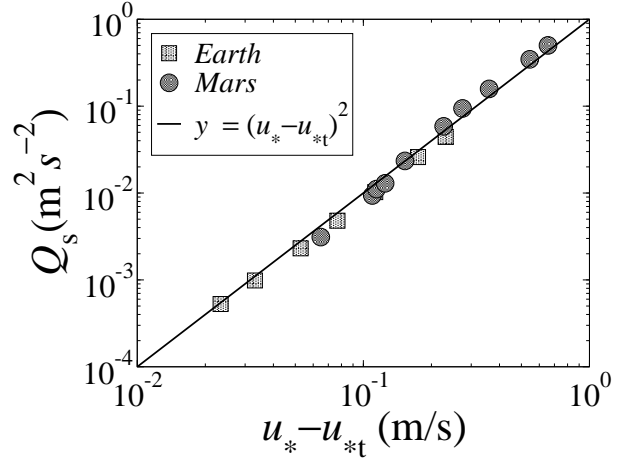


**FIGURE 3.** Normalized flux  $Q_s$  defined as  $q_s / [227.3 \cdot u_{*t} \cdot d \rho_{\text{fluid}}^{5/3} / (\eta g)^{2/3}]$ . Circles and squares correspond to calculations made for Mars and Earth, respectively. The straight line corresponds to the equation  $y = (u_* - u_{*t})^2$ .

from the sand bed.

As compared to Earth trajectories, Martian saltation paths are giant. While Earth saltating particles do not exceed heights of 15 cm, maximum heights reached by particles saltating under typical sand-moving winds on Mars (fig. 1) amount to 1 – 5 m. Moreover, Martian grains saltate in 20 – 120 m long paths — such particles appear rather suspended when seen in a wind tunnel with length of a few meters [4]. The simulation results are in agreement with the expectation that the saltation length  $L_{\text{salt}}$  should scale with the quantity  $L_{\text{drag}} = d \rho_p / \rho_{\text{fluid}}$ , which is a characteristic length that encodes the information of the inertia of a saltating grain in the surrounding fluid [18].

## DISCUSSION AND CONCLUSION

How can the simulation results presented here be helpful for the understanding of dune formation on Mars? Whether dunes could be formed at present atmospheric conditions of Mars remained in fact an open question for decades since the first images of Mars dunes taken by Mariner 9 [1, 19]. Noticeable changes on the surface of a few Martian dunes have been detected only recently (e.g. as reported in refs. [20]). These observations provided evidence that dunes can be formed and move on the present Mars. However, since the wind velocity is seldom above the threshold for saltation motion on Mars, the rate at which changes on the dunes occur is so low that no dune migration could be detected from orbiters up to now.

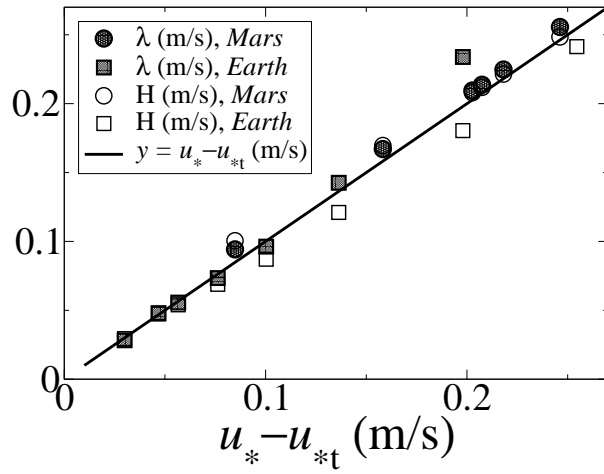


**FIGURE 4.** Universal expressions for saltation transport — The normalized length  $\lambda \equiv L_{\text{salt}}/[1091.5 \cdot (l_v/\sqrt{gd})]$  and height  $H \equiv H_{\text{salt}}/[81.46 \cdot (l_v/\sqrt{gd})]$  as function of  $u_* - u_{*t}$ , are shown by the full, respectively by the empty symbols, both for Mars (circles) and Earth (squares), with  $u_{*t} = 1.03$  m/s and  $0.244$  m/s for Mars and for Earth, respectively. All data seem to follow the straight line,  $y = u_* - u_{*t}$ .

In conclusion, the present work reported the first calculation of particle trajectories in a turbulent wind. The sand flux, saltation height and length on Mars and on Earth were studied and general expressions (eqs. (4), (5) and (6)) were found which can be applied in order to calculate these quantities under different physical conditions, e.g. on the surface of Venus or Titan. The giant saltation trajectories and the high grain velocities on Mars are the missing link to understand the triggering of dust storms under typical wind velocities  $u_* \approx 1.0$  m/s at present conditions of Mars [2].

The large values of impact velocities obtained in the simulations allow us to understand the high erosion of Martian soils during the rare gusts of sand transport as predicted from wind tunnel simulations of saltation under low-pressure conditions that reproduce the density of the Martian air [2] and from experiments of particle-bed collisions under typical conditions of grain velocity on Mars. It would be interesting to extend the calculations of the present work in order to study the development of saltation from the initiation of transport by aerodynamic (direct) entrainment, with inclusion of a splash function that accounts for the response of the number of ejected grains with respect to the impact velocity of saltating particles.

## ACKNOWLEDGMENTS

This work was supported in part by CNPq, CAPES and FUNCAP (Brazilian Agencies) and by Volkswagens-

tiftung and The Max-Planck Prize.

## REFERENCES

1. McCauley JF (1973) Mariner 9 Evidence for Wind Erosion in the Equatorial and Mid-Latitude Regions of Mars. *Journal of Geophysical Research* 78:4123-4137.
2. Greeley R (2002) Saltation impact as a means for raising dust on Mars. *Planetary and Space Science* 50:151-155.
3. Bagnold RA (1941) *The physics of blown sand and desert dunes* (Methuen, London).
4. White BR (1979) Soil transport by Winds on Mars. *Journal of Geophysical Research* 84:4643-4651.
5. Anderson RS, Haff PK (1988) Simulation of eolian saltation. *Science* 241:820-823.
6. Greeley R, Leach R, White B, Iversen JD, Pollack J (1980) Threshold windspeeds for sand on Mars: Wind Tunnel Simulations. *Geophysical Research Letters* 7:121-124 (1980).
7. Iversen JD, White BR (1982) Saltation threshold on Earth, Mars and Venus. *Sedimentology* 29:111-119.
8. Sullivan R, Greeley R, Kraft M, Wilson G, Golombek M, Herkenhoff K, Murphy J, Smith, P (2000) Results of the Imager for Mars Pathfinder windsock experiment. *Journal of Geophysical Research* 105:24547-24562.
9. White BR, Greeley R, Iversen JD, Pollack JB (1976) Estimated grain saltation in a Martian atmosphere. *Journal of Geophysical Research* 81:5643-5650.
10. Lettau K, Lettau H (1978) in *Exploring the World's Driest Climate*, eds Lettau H, Lettau K (University of Wisconsin, Madison), pp 110-147.
11. Durán O, Herrmann, HJ (2006) Modellization of saturated sand flux. *J Stat Mech* P07011.
12. Almeida MP, Andrade JS, Jr, Herrmann HJ (2006) Aeolian transport layer. *Physical Review Letters* 96:018001.
13. The FLUENT (trademark of FLUENT Inc.) commercial package of fluid dynamics is used in this study.
14. Morsi SA, Alexander AJ (1972) An investigation of particle trajectories in two-phase flow systems. *J. Fluid Mech.* 55:193-208.
15. Rioual F, Valance A, Bideau D (2000) Experimental study of the collision process of a grain on a two-dimensional granular bed. *Physical Review E* 62:2450-2459.
16. Kroy K, Sauermann G, Herrmann HJ (2002) Minimal model for sand dunes. *Physical Review Letters* 88:054301.
17. Greeley R, Blumberg DG, Williams SH (1996) Field measurements of the flux and speed of wind-blown sand. *Sedimentology* 43:41-52.
18. Andreotti B, Claudin P, Douady S (2002) Selection of dune shapes and velocities Part 1: Dynamics of sand, wind and barchans. *Eur Phys J B* 28:321-339.
19. Breed CS, Grolrier MJ, McCauley JF (1979) Morphology and distribution of common 'sand' dunes on Mars: Comparison with the Earth. *Journal of Geophysical Research* 84:8183-8204.
20. Bourke MC, Edgett K, Cantor BA (2008) Recent aeolian dune change on Mars. *Geomorphology* 94:247-255, doi:10.1016/j.geomorph.2007.05.012.
21. Parteli EJ, Herrmann HJ (2007) Dune formation on the present Mars. *Physical Review E* 76:041307.